

Gap states in non-crystalline selenium: roles of defective structures and impurities

K. TANAKA

Department of Applied Physics, Graduate School of Engineering, Hokkaido University, Sapporo Kita-ku, 060-8628, Japan

After briefly reviewing electronic properties governed by gap states in amorphous and glassy Se, we consider the responsible structures through empirical and ab-initio molecular-orbital calculations. So far many fundamental and application-oriented studies on Se have been performed, respectively, for melt-quenched glasses and evaporated amorphous films, while the atomic structures producing gap states still remain vague. The calculation for Se clusters such as H- n Se-H demonstrates that variations of dihedral angles and inter-cluster separations bring substantial fluctuations in the HOMO energy, which may cause hole traps in solid Se. The LUMO energy varies with n , which suggests that long ($n \geq 5$) chain segments behave as electron traps. Small rings and dangling bonds create several gap-states, which may work as traps and absorption centers. For extrinsic defects, oxygen effects have been emphasized. The calculation demonstrates that O atoms behave as potent isoelectronic impurities, being negatively charged, making nearest-neighbor Se atoms positive. Such an ionic pair can produce a deep LUMO level, which possibly works as an acceptor. Compensation effects of As (and Si) into O-contaminated Se are ascribed to the production of stronger As(Si)-O bonds, which are electrically inactive due to wider HOMO-LUMO gaps.

(Received September 17, 2015; accepted October 28, 2015)

Keywords: Amorphous, Selenium, Oxygen, Gap-state, Defect, Impurity

1. Introduction

Se has been utilized as a semiconductor for the longest time since the inventions of photocells and rectifiers consisting of crystalline layers in the early 20th century [1]. We then devised a-Se (a- for amorphous) xerographic photoreceptors [1-4]. And, the film has been developed to *avalanching* photoconductive targets in vidicons and x-ray conductors in flat-panel imagers [4-7]. In addition, Se nano-wires attract considerable interest recently [8-11]. We also note that Se, being situated between S and Te in the periodic table [12], solidifies into several crystalline allotropes and notably into only-one monatomic glass which is fairly stable at room temperature [1, 13].

These backgrounds have prompted a lot of scientific studies, which uncover fundamental features of Se [1-4]. In all of the condensed phases, the atomic bond is governed by the s^2p^4 electron configuration, giving rise to two-fold coordinated covalent bonds and lone-pair (LP) electrons with π -type wavefunctions, which forms aligned helical chains in trigonal Se and stacked rings in monoclinic Se. In non-crystalline Se, the structure may be composed with mixtures of entangled chains and distorted rings [1-4, 14, 15], the ratio possibly depending upon preparation procedures and prehistory of specimens. On the other hand, in all of the allotropes, the two-fold coordinated atomic structure governs electronic properties as semiconductors, with the valence and conduction bands consisting of LP and anti-bonding states, which are separated by optical gaps E_g with widths of ~ 2 eV. It has also been known that, in crystalline and amorphous Se, holes are much more mobile than electrons [1-4, 12, 16-18].

However, defective structures and impurity effects remain largely elusive. The concept of charged dangling bonds (and valence alternation pairs) D^+ and D^- , proposed for chalcogenide glasses [19,20], has repeatedly been employed [2-4], while the existence cannot be substantiated. This is because we have no experimental tools which can identify the point-defective structure having *paired* electron spins. Also, numerical calculations, which examine electronic states of amorphous, liquid and molecular Se from various standpoints [21-35], have given diverse or controversial results. And, other defective structures such as LP/LP interactions [36], polarons [26], and four-fold coordinated Se [31, 32] have been proposed. In addition, dramatic effects of O impurities remain puzzling, which may be responsible for all the defect-related properties in a-Se [37], while no detailed analyses have been reported.

In the present work, after briefly reviewing notable observations of defect- and impurity-related electronic properties in Se, we consider the structural origins through simple molecular-orbital calculations. Since the overall non-crystalline structure seems to be intricate to be grasped, we analyze the role of elemental atomic structures one-by-one. A variety of structural components are evaluated for Se(:H:O:As) clusters under the same formulations, which can afford relative comparisons of obtained quantities. The present study will give fundamental insight into the gap state in a-Se, the understanding being prerequisite for further developments of photoelectronic devices.

2. Observations

Previous studies on the gap state in Se may be divided into the two, which does or does not take O-impurity effects into account. Historically, oxygen effects seemed to be first noticed in polycrystalline Se [38, 39], then in liquid Se [40], g-Se (g- for melt-quenched glassy) [41], and finally in a-Se films [42,43], the sequence following the development of devices from crystalline Se photocells to a-Se photoreceptors. Here, we should note two kinds of difficulties, which may cause non-reproducible results presented hereafter.

One concerns the purity. For preparing samples, many experiments employ Se pellets with nominal purities of 5N – 6N, which are evaluated in general only for metallic atoms [42,44,45], with the concentrations of light atoms such as O having rarely been specified. Otherwise, some problems seem to exist in the evaluation of O contents. Actually, Burley [46] faced poor reproducibility in infrared spectroscopy detections of 100ppm-level O in g-Se. (The fractional unit “ppm” has often been used without specifying its unit, which may be weight or number, while the latter seems to be more common [46]. Note that the atom-number density of 10^{16} cm^{-3} corresponds ~ 1 ppm.) Other studies reported that minimal O contents evaluated by infrared spectroscopies are ~ 500 ppm [47] and 10^{-4} wt.% (≈ 5 ppm) [48], and by ion-mass analyses ~ 20 ppmw (~ 100 ppm) [49]. These results suggest that it is difficult to know the O density below $\sim 10^{17} \text{ cm}^{-3}$, which is substantially worse than that ($\sim 10^{15} \text{ cm}^{-3}$) in crystalline Si wafers. Note that this O density is comparable to that, $\sim 10^{16} \text{ cm}^{-3}$, estimated for the charged defect in a-Se [2-4].

The other is the existence of a variety of samples, the fact which originates from the quasi-stability inherent to non-crystalline solids. Specifically, it is highly plausible that g- and a-Se exhibit substantially different properties. We may envisage that a glassy sample, obtained through melt-quenching procedures, is dominated by constituents of the liquid, i.e., chain molecules [1]. On the other hand, a-Se films deposited on to substrates held at some temperatures are obtained from Se gas, which probably consists of short chains and small-ring clusters [50-53]. It is then plausible that the glass property is relatively uniquely-fixed, which may be appropriate to fundamental studies. By contrast, the film is likely to be more unstable with varied properties, and accordingly, the properties become necessarily diverse, making the characterization difficult. For instance, to the author’s knowledge, dependence of the resistivity on the O content has not been reported for a-Se. Actually, nominally-pure films exhibit scattered values extending over $10^{12} - 10^{16} \Omega\text{cm}$ [54-58]. We should also take care that the quasi-stability causes marked structural relaxation. For instance, O-related aging effects have been detected in infrared spectra of g-Se [46, 47, 59] and transport properties in a-Se [60].

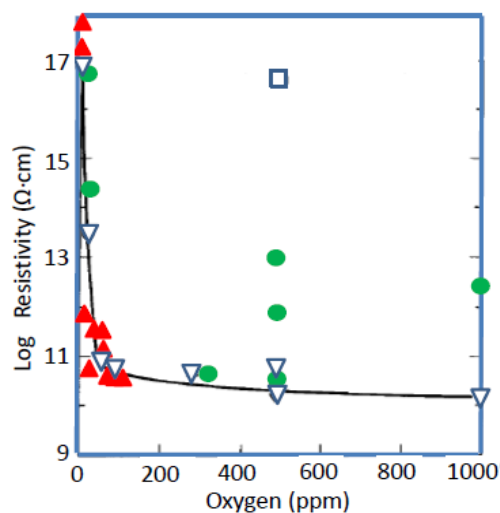


Fig. 1. Resistivity of g-Se as a function of oxygen content; reported in [59] (∇ with a solid line), [47] (\bullet), and [62] (\blacktriangle). The square (\square) at upper middle shows a result of g-Se co-doped with 500ppm SeO_2 and 500ppm Si [59].

In addition, another factor has given additional complications to the film property. As known, pure a-Se films are likely to crystallize [1] so that many application-oriented studies have dealt with the so-called “stabilized a-Se films” containing 0.2 – 0.5 wt.% As (and ppm-level Cl etc.), which are prepared by evaporation onto substrates held at $\sim 60^\circ\text{C}$ [34,58,60]. However, influences of the dopants upon electronic properties have not necessarily been understood fully.

2.1. Pioneering work

It has repeatedly been demonstrated since the 1950s that the electrical resistivity in various forms of Se [1,2,61] dramatically decrease with O contaminations. In particular, as shown in Fig. 1, the resistivity in g-Se decreases by 6 – 7 orders of magnitude with inclusion of only ~ 10 ppm O, while further O additions seem to hardly affect the value. Kozyrev [39] suggested on the basis of thermo-power measurements that the resistivity decrease is caused by creation of acceptor levels. Twaddell et al. [62] connected the resistivity decrease with a decrease in the electrical activation energy from ~ 1.2 to ~ 0.6 eV, while McMillan and Shutov [63] obtained a fixed value of ~ 0.9 eV.

It may be valuable to mention here two effects induced by other atoms. One is that the O-related resistivity decrease can be compensated by addition of some elements such as As and Si [47,59,63]. For instance, as shown in Fig. 1, Si and O co-doping to g-Se yields nearly the same resistivity with that of pure samples. The other is that incorporations of S and/or Te, instead of O, into a- and g-Se give much smaller effects [18,55,64-67].

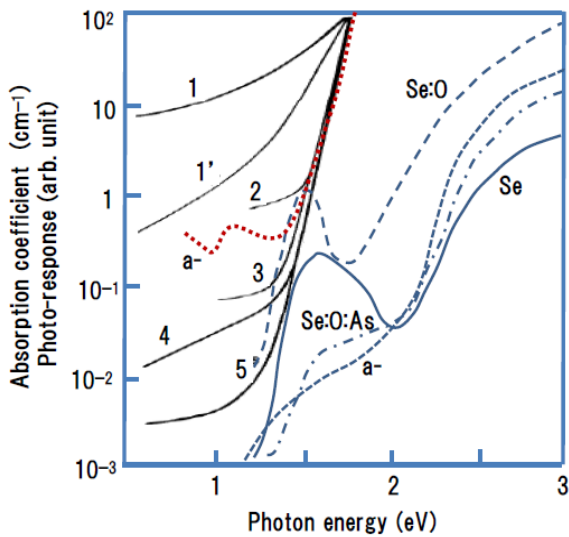


Fig. 2. Variations of optical absorption (left-hand part) [68] and photoconductivity (right-hand part) [63] spectra in g-Se with purification and doping. The absorption reduces with purification from 1 to 5. In the photoconduction spectra, "Se" refers to 6N-purity g-Se, "Se:O" to one doped with 250ppm O, and "Se:O:As" to one doped with 250ppm O and 250ppm As. Also shown by "a-" are absorption and photoconductivity spectra of nominally-pure amorphous Se films [70,71].

A few groups have studied purity-dependent spectral variations around the optical absorption edge. As shown in Fig. 2, Vaško et al. [68] demonstrated for g-Se that residual absorption below the Urbach edge, at $\hbar\omega \approx 1.0$ eV, decreases with purification. (However, if the change corresponds to the O concentration is not inferred.) Also shown in the figure are photoconductivity spectra in g-Se [63], in which the solid line denotes the one of nominally-pure samples. We see here the so-called non-photoconducting spectral gap [1-4,69]; the photoconductivity spectral edge being blue-shifted from the absorption edge, and also a broad peak at ~ 1.6 eV, which is attributable to residual crystallites [70]. Then, addition of 250ppm O causes an overall photoconductivity increase of an order of magnitude with a conspicuous peak at ~ 1.5 eV. And, As co-doping seems to suppress these changes. Note that the spectral regions of the residual absorption (~ 1.0 eV) and the photoconductivity peak (~ 1.5 eV) do not overlap, so that the roles of O atoms in these spectral results remain unclear. Incidentally, as plotted by dotted lines in Fig. 2, nominally-pure a-Se films present similar, but different, absorption and photoconduction spectra [70,71].

Spin-related characteristics have also been explored. Pioneering studies demonstrated that ESR behaviors in crystalline (which may be damaged) and g-Se appear to be similar, ascribing the signals to chain-terminating O atoms [72-74]. Ablullaev et al. [72] mentioned that, in nominally-pure Se, the O-related spin density does not exceed 10^{17} cm^{-3} . Abkowitz [75] asserted the non-existence

of chain-end Se spin signals. Later experiments [76,77] evaluated the density of unpaired spins in nominally-pure g-Se to be, at most, $10^{15} - 10^{16} \text{ cm}^{-3}$. These values seem to be in harmony with a viscosity study, which suggests that liquid Se at the melting temperature consists of chains longer than $10^5 - 10^6$ atoms [78], giving rise to the density of chain ends of $10^{16} - 10^{17} \text{ cm}^{-3}$. Little or non-detectable unpaired electron spins may imply little gap states, which is consistent with photoemission results that demonstrate un-pinned Fermi levels in a-Se films, which were deposited onto substrates held at 25 [79] and 50 °C [80].

2.2. Studies after 1975

As known, Street and Mott [19] and successively Kastner et al. [20] presented the charged defect models for chalcogenide glasses, which have exerted strong influences upon later studies [2-4]. Bishop et al. [81] manifested the existence of optically-induced ESR centers in g-Se at 4 K, which were interpreted as neutral D^0 that is photo-transformed from D^+ and/or D^- . The spin density suggested the number of the charged defects in g-Se to be $\sim 10^{16} \text{ cm}^{-3}$, which is an order of magnitude smaller than those in $\text{As}_2\text{S}(\text{Se})_3$ [2,81]. Later, Kolobov et al. [82] have demonstrated for a-Se films at 20 K that the photo-induced spin density increases up to 10^{20} cm^{-3} , which they ascribed to singly- and triply-coordinated Se defects. The charged defect models were employed also for interpreting photoluminescence behaviors [83], including its emission spectrum at $\sim E_g/2$ and the so-called photoluminescence fatigue under prolonged illumination. Following these studies, several groups have estimated energy depths of the defect states using thermally-stimulated currents [84] and transient photocurrent experiments [85,86]. However, it is plausible that these defect-related properties are affected by structural relaxation and impurities.

Actually, a few groups have examined the effect of O impurities upon photoluminescence in g-Se. Spectral studies demonstrated that the excitation and emission spectra are mostly insensitive to the O doping [83,87,88]. On the other hand, luminescence intensity decreased with the O contents, at different O levels of 1 at.% [83] and 10^{-3} wt.% (= 0.05 at.% = 500ppm) [88]. Kolomiets et al. [88] also reported that the fatigue became more prominent in O-denser samples. No interpretations seem to be given to these observations.

Doping effects on photo-carrier transport have also been investigated for a-Se films [2,42,43,60]. As exemplified in Table 1, for pure films, which were deposited onto substrates held at temperatures of ~ 60 °C, all the studies present roughly the same values for the drift mobility of holes and electrons; 0.15 and $0.005 \text{ cm}^2/\text{Vs}$ [2,18,42,60,64]. In addition, as indicated by the arrows in the table, it seems that the O doping (or treatment) does not affect the hole mobility [42,43,60], which means that no

O-related changes occur in shallow hole-trapping centers. For the hole lifetime, however, Oda et al. [42] and Belev et al. [60] present opposite changes, decrease and increase, with the O doping. Since the electrical conduction Se is undoubtedly governed by holes [1-4], the increase in the hole lifetime reported by Belev et al. [60] for a-Se may be consistent with the overall photoconductivity enhancement in g-Se [63] (Fig. 2). For electrons, both the results [42,60] manifest a fixed mobility below ~10 ppm O and gradual lifetime decreases with the O density, which are ascribable to formation of deep traps. However, quantitative behaviors in these two studies appear substantially different. Finally, it should be mentioned that if we could compare these results in a-Se with those in g-Se, in forms of squeezed or polished layers, more valuable insights would be obtained.

Table 1. Drift mobilities μ (cm^2/Vs) and lifetimes τ (μs) of holes (h) and electrons (e) in pure and O-doped a-Se films. The arrows indicate the changing directions induced by the O doping. In Odas' results, all the properties are the same in undoped and 100-ppm O-doped samples, while Belevs' detect some differences between in undoped and 7-ppm O-doped samples.

material	μ_h	τ_h	μ_e	τ_e	Reference
pure	0.14	10~50	0.006	50	Schottmiller [64]
pure	0.15	50	0.007	~10	Gill [18]
pure (~100ppm)	~0.15	10	0.005	150	Oda [42]
+1000ppm O	~0.15 →	~5 ↘	0.005 →	~50 ↘	
pure (\leq 5ppm)	0.15	~10	0.005	~500	Belev [60]
+50ppm O	0.13 →	390 ↗	trap ↘	~10 ↘	

3. Calculation

Electronic states in a variety of small Se clusters have been studied through quantum chemical calculations. Softwares utilized are semi-empirical and ab initio packages, MOPAC-PM3 [89] and GAMESS [90], which are operated on a visualization platform of Winmostar V5 [91]. For paired- and unpaired-spin clusters, we adopt the spin-restricted and unrestricted approximations. In the ab initio calculations, after some trials, the 6-31+G* basis set has been employed, in combinations with the HF (Hartree-Fock) method and the DFT (Density Functional Theory) with B3LYP (Becke's three-parameter hybrid exchange functional and the Lee-Yang-Parr) correlation function, which have been demonstrated to give satisfactory agreements to experimental parameters of various molecules [92]. Note that the empirical and the ab initio calculations evaluate molecular states, respectively, at room temperature and 0 K. It should also be noted here that the dielectric constant in bulk samples is implicitly neglected in these molecular-based calculations.

All these programs could afford cluster structures and the electronic energies which are comparable with those obtained by experiments [1,53,93-99] and previous numerical calculations [25,94,97,100-104]. For instance, Table 2 compares fundamental parameters of the listed molecules obtained by the three procedures with the reported. Quantitatively, as tabulated, the HOMO-LUMO gap of a cluster tends to decrease in the order of HF, PM3 and DFT, with the difference becoming more conspicuous in larger clusters (see, Fig. 6). The calculation times of PM3, HF, and DFT methods were roughly in the ratio of 1: 10^3 : 2×10^3 . However, it should also be mentioned that PM3 tends to give unreasonable results for clusters having unpaired electrons. In short, it is difficult to select the most appropriate method to the present analyses, and accordingly, we will employ those on a case-by-case basis.

Table 2. Structural and electronic parameters in the three molecules, obtained by the present calculations (first line), previous calculations (second line), and experiments (third line). The present results, the structure being optimized in energy-minimization routines, are listed in the order of PM3, HF and DFT. The third and fourth columns compare sign-reversed HOMO and LUMO energies with experimental ionization potential IP and electron affinity EA [92].

	Bond length [Å]	Bond angle [°]	-HOMO/IP [eV]	-LUMO/EA [eV]	H-L GAP [eV]
Se ₂	2.14, 2.23, 2.20	–	8.8, 8.4, 5.7	4.2, 1.7, 1.4	4.6, 6.7, 4.3
	2.1~2.2 [25,101,104]		~8.7 [104]	~2.0 [102-104]	~6.7
	2.2 [1]		~8.8 [93,53]	1.9 [95]	~6.9
HSe	1.47, 1.45, 1.49	–	9.1, 9.5, 9.5	2.3, 0.1, 0.4	6.8, 9.4, 9.1
	~1.46 [25, 94]		~9.9 [25,100]		
	1.47 [25]		9.8 [94,99]	2.2 [99]	7.6
H ₂ Se	1.47, 1.46, 1.48	94, 93, 91	9.8, 9.7, 6.7	0.6, -1.5, 0.6	9.2, 11.2, 6.1
	1.46 [96, 97]	~90 [96, 97]	9.8 [25, 97, 100]	0.3 [97]	9.5
	1.46 [1, 96, 97]	91 [1]	9.9~10 [98, 99]		

Fig. 3 shows a helical H-15Se-H cluster obtained using the HF procedure. The structure has a bond length $r \approx 2.33$ Å, bond angle $\theta = 105^\circ$, and dihedral angle $\varphi = 81^\circ$ for the Se sequence, which are comparable with previous results of single Se chains [9, 24, 25] and Se solids [1-3,105]. The HOMO and LUMO levels, originating from π^* and σ^* states, are located at -9.0 eV and +0.4 eV (Fig. 6), giving rise to a HOMO-LUMO gap of 9.4 eV, which is appreciably higher than the gap 4.7 eV obtained by PM3, 3.5 eV by DFT, ~3 eV in a previous calculation [25], an optical gap of ~2.5 eV of single Se chains in a zeolite ZSM-5 [9], and the band gap of ~2.0 eV in solid Se [1,2]. Incidentally, the work function in a-Se is reported to be ~6 eV [79, 80].

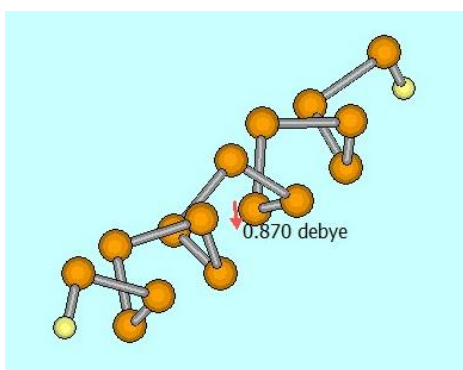


Fig. 3. An energy-minimized helical H-15Se-H, obtained by the HF calculation.

4. Results and Discussion

4.1. Disordered chains

It is known that the radial distribution function of a-Se possesses clear first and second neighbor peaks, but the

third peak merges into the background [1, 2, 4, 105]. This observation evinces nearly-fixed bond length r and angle θ , with disorder in the dihedral angle φ . Hence, it may be straightforward to examine first the varied φ effect on electronic states.

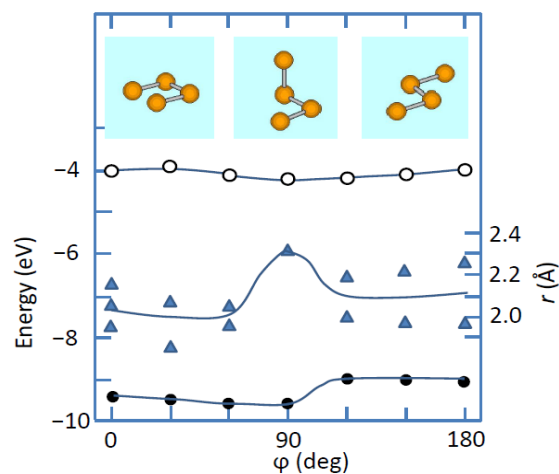


Fig. 4 Variations of the HOMO (●) and LUMO (○) energies and the bond length r (▲) as a function of the dihedral angle φ in a H-4Se-H chain with $\theta = 100^\circ$. In some configurations, r in the central and edge bonds are different, which are denoted by two or three triangles. The insets illustrate schematic Se structures with $\theta = 90^\circ$ and $\varphi = 0, 90$ and 180° .

Fig. 4 shows the result for a H-4Se-H chain evaluated using PM3. Note that similar results have been obtained by the HF and DFT methods. We see that the variation of φ modifies electronic energies and also r . In detail, the

HOMO energy varies by ~ 1 eV (~ 2 eV in HF and DFT) with a minimum at $\varphi \approx 90^\circ$, while the variation of the LUMO energy is much smaller.

These contrasting behaviors reflect different level characters [1-4]. The HOMO state in single chains is affected by intra-chain interaction between π^* orbitals, which varies with φ . For instance, in the planar zig-zag structure with $\varphi = 180^\circ$, the paralleled LP wavefunctions provide the strongest interaction, and accordingly, the structure gives the highest HOMO level [23-25]. (At $\varphi = 0^\circ$, interaction between the end Se atoms adds a small σ -bond effect.) On the other hand, in the helical configuration of $\varphi \approx 90^\circ$, the intra-chain LP/LP interaction is the weakest, which tends to loosen the covalent bond, giving rise to the r increase, and lowers slightly the LUMO level consisting of σ^* states. It can therefore be envisaged that in a-Se the dihedral-angle disorder causes shallow traps for holes.

Next, taking the different origins of the HOMO and LUMO states, we assume that the HOMO energy is sensitive also to the inter-cluster separation R [1-4]. Actually, PM3 calculations for two planar H-2Se-H clusters, which are stacked in parallel (Fig. 5), have demonstrated that compaction of R from 5 to 3 Å monotonically raises the HOMO level from -8.9 to -7.9 eV (by 1.0 eV) while the LUMO level is nearly fixed (< 0.1 eV) at -3.6 eV. Similar results have been obtained by HF and DFT, in which the corresponding changes in the HOMO levels amount to 1.8 and 1.5 eV. Accordingly, disordered R in a-Se also causes traps for holes, limiting its drift mobility.

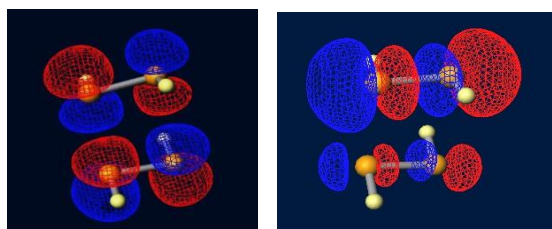


Fig. 5. Wavefunctions of HOMO (left) and LUMO (right) states in parallel-positioned two planar H-2Se-H clusters with an inter-cluster separation R of 3.5 Å.

In contrast to these marked effects of φ and R upon the HOMO level, the LUMO level is substantially affected by the length n of helical chains H- n Se-H. We see in Fig. 6 that all the calculations manifest fairly stable HOMO levels at around -6 (in DFT) and -10 eV (in PM3 and HF). The calculations have also demonstrated that the energy-optimized chain geometry with $r \approx 2.34$ Å, $\theta \approx 106^\circ$ and $\varphi \approx 82^\circ$ hardly changes with n . Nevertheless, the lengthening of H- n Se-H from $n = 1$ to 6 markedly lowers the LUMO energy by 1 – 4 eV, causing substantial HOMO-LUMO gap narrowing, in consistent with a previous semi-empirical calculation [25]. Such a characteristic difference of the HOMO and LUMO behaviors can be interpreted as the result of a periodic

structure effect, which appears more prominently in coupled σ^* states of the LUMO level.

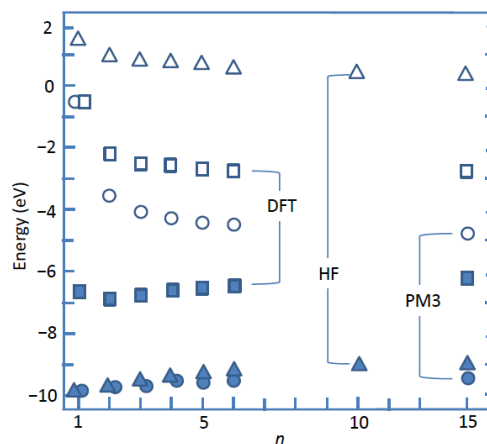


Fig. 6. HOMO (solid symbols) and LUMO (open symbols) energies of helical H- n Se-H chains as a function of n . The results are obtained by PM3 (\bullet, \circ), HF ($\blacktriangle, \triangle$) and DFT (\blacksquare, \square).

Accordingly, the chain disordering seems to cause an interesting consequence. Provided that non-crystalline Se consists of segmental chains with varied atom numbers ($n \geq 2$), which are connected through kinks, long segments (wide potential wells) can work as electron traps. For instance, a PM3 calculation has demonstrated that in the bent H-15Se-H chain shown in Fig. 7, which consists of four helical segments connected with cis-configurations, modifications of the LUMO and the HOMO energies are, respectively, ~ 0.2 eV and less than 0.1 eV.

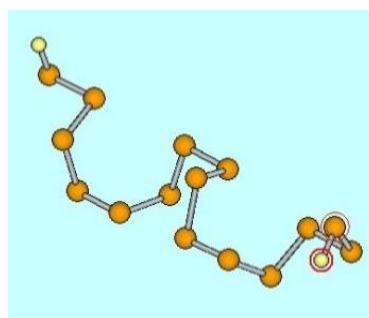


Fig. 7. A distorted H-15Se-H chain, containing four alterations of $\theta = -100^\circ$, from that in Fig. 3.

4.2. Rings

It is plausible that a-Se films, specifically which are deposited onto low-temperature substrates, contain substantial numbers of ring molecules [1]. Fig. 8 compares the HOMO and LUMO energies of Se_n rings, evaluated using the energy-optimized (minimal electronic energy) DFT, with those of helical H- n Se-H chains (Fig. 6). We see narrower HOMO-LUMO gaps in the small rings with $n = 3 \sim 5$, in which Se_3 has an equilateral triangular shape with $r \approx$

2.40 Å while Se_4 and Se_5 appear to be non-planar (with $\theta \leq 100^\circ$ and $\varphi \approx 40^\circ$), which are compared with previous results [33, 101-104, 106, 107]. The total energies of these rings are higher by ~ 0.5 eV/atom than those of greater rings ($n \geq 6$) [33,104,107], and such strains may cause the narrower gaps. On the other hand, the greater rings with $n = 6$ and 8 are crown-shaped with $r \approx 2.37$ Å, $\theta \approx 105^\circ$ and $\varphi \approx \pm 109^\circ$, the geometry giving rise to similar HOMO and LUMO energies to those of the helical chains. Hence, if small rings (or nearly-closed chains as that in the central part in Fig. 7) are included in a-Se matrices, the localized structures may produce gap states both for electrons and holes.

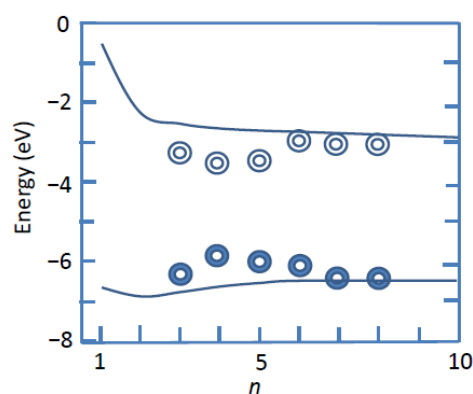


Fig. 8 HOMO (lower) and LUMO (upper) energies of Se_n rings (double circles), which are compared with those (solid lines) in H-nSe-H helical chains (Fig. 6).

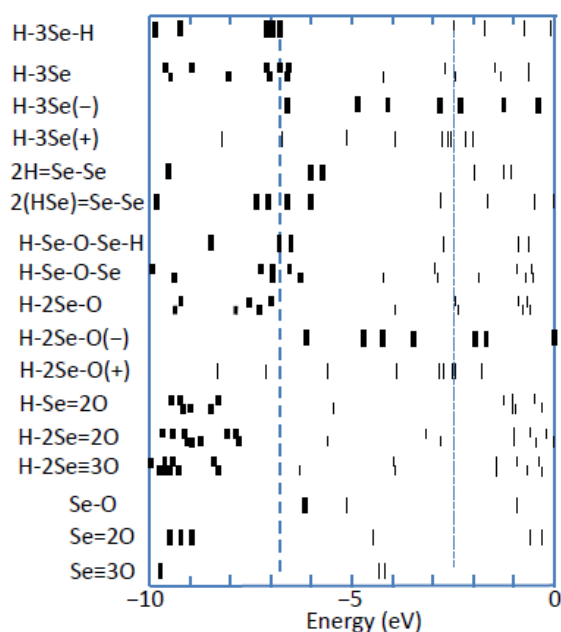


Fig. 9. Occupied (thick bar) and un-occupied (thin bar) levels of the clusters indicated, calculated by the energy-optimized DFT. For un-paired spin systems such as H-3Se , the bar length is reduced, representing single electron states. The dashed lines extend the HOMO and LUMO levels in H-3Se-H at -6.8 and -2.5 eV.

4.3. Defective structures

4.3.1. Dangling bonds

Fig. 9 compares electronic energies of dangling bonds with those in helical H-3Se-H , the results being obtained using DFT. The length $n = 3$ is selected here, since it represent behaviors in longer chains (see Fig. 6), while calculations for some clusters with $n = 5$ have provided qualitatively similar results. It should be mentioned here that, for H-nSe clusters having an unpaired electron, PM3 tended to provide erroneous results: the spin eigenvalue s , which should satisfy $s^2 = 0.75$ for doublets, increased with n , from 0.77 to 3.3 for $n = 1$ to 4, which was retained in stable values of $0.75 - 0.77$ in HF and DFT calculations.

We see in the figure that H-3Se , containing a neutral dangling bond (D^0, C_1^0), gives a LUMO state at around -4 eV, or ~ 2.5 eV above the HOMO level of H-3Se-H . This mid-gap state has a π^* -type wavefunction, the energy being raised by LP/LP interaction between the end and the next-to-end Se atom [21,26], which is enhanced by the paralleled wavefunctions and a shorter bond distance of 2.26 Å than that (2.34 Å) between the second and the third atom. Provided that such a neutral dangling bond exists in Se solids, the state may work as a deep electron trap and an optical absorption center. It is plausible that this unpaired spin is responsible for ESR signals appearing in photo-excited g-Se [81] and a-Se [82]. Nevertheless, to the author's knowledge, no corresponding mid-gap absorption has been reported for non-crystalline Se.

On the other hand, Fig. 9 shows that the charged clusters having dangling bonds, $\text{H-3Se}(\pm)$, exhibit multiple gap-states, which are totally occupied in $\text{H-3Se}(-)$ and unoccupied in $\text{H-3Se}(+)$. Such features seem to reflect Coulombic potentials [26], and actually, the bond distance r at the end atoms changes (from 2.26 Å in H-3Se) to 2.33 and 2.18 Å in $\text{H-3Se}(-)$ and $\text{H-3Se}(+)$. The negative and positive charges repulse (raise) and attract (lower) the occupied and unoccupied states (levels), and accordingly, these may behave as traps for holes and electrons, respectively.

However, the existence, or the concentration, naturally depends on the total energy. We here compare stabilized total energies of the two systems having an identical number of electrons; one being H-6Se-H and the other being an isolated pair of $\text{H-3Se}(-)$ and $\text{H-3Se}(+)$, which possess -14408.25 and -14407.98 H (1 H = 27.2 eV), i.e. the latter being higher (more unstable) by 0.27 H (≈ 7 eV). In real a-Se matrices, such an energy difference may be reduced by the relative dielectric constant of ~ 6 [1,3], while the difference is still greater than 1 eV, which gives a thermal factor of $\exp(-1\text{eV}/k_B T_g) \approx 10^{-15}$, where the glass-transition temperature $T_g \approx 310$ K [1,3]. Accordingly, in consistent with previous predictions [21,22], the D^- and D^+ defects are unlikely to exist in a-Se.

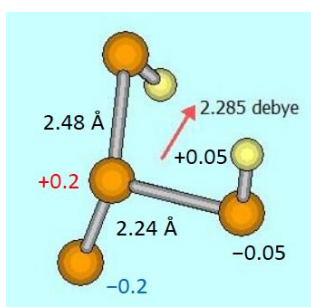


Fig. 10. An energy-minimized $2(\text{SeH})=\text{Se}-\text{Se}$ cluster with polarization, Mulliken atomic charges, and two bond lengths.

4.3.2. Three-fold coordinated defects

Does a three-fold coordinated Se atom exist in a-Se? Structure optimization of $\text{Se}\equiv 3(\text{SeH})$ by the spin-unrestricted DFT has demonstrated that the cluster decomposes to a H-3Se-H chain and a Se-H fragment, which suggests that the so-called C_3^0 is energetically unfavorable. It seems that ion-ion repulsion cannot retain the three-folded Se structure [21].

However, the calculation has suggested other possibilities. The $2\text{H}=\text{Se}-\text{Se}$ (and also $2(\text{SeH})=\text{Se}-\text{Se}$ in Fig. 10) cluster, having three- and one-fold (C_3 and C_1) coordinated atoms, is stable with the three- and the one-folded Se being charged positively and negatively; the atomic pair may be regarded as an IVAP (intimate valence alternation pair) [20,26]. The total energies are higher only by ~ 1 eV than those in the corresponding helical chains H-2Se-H (and H-4Se-H). Provided that the energy reduction by the dielectric constant could work in such an atomic scale, the concentration ratio of the pair to the helical chain amounts to 10^{-3} . And, as shown in Fig. 9, such clusters tend to possess HOMO states with localized π^* wavefunctions just above (by ~ 1 eV) the reference HOMO level. These results suggest that appreciable IVAPs can exist, which may work as hole traps. Here, it would be valuable to mention that $2\text{H}=\text{Se}-\text{Se}-\text{Se}$ has decomposed to $2\text{H}=\text{Se}$ and 2Se , the fact implying that the C_3^+ and C_1^- should form a nearest-neighbor pair.

4.4. O impurity

Fig. 9 also compares electronic levels of several structures which contain oxygen. O atoms may be included in Se matrices in two ways; one being incorporated into Se clusters such as $-\text{Se}-\text{O}-\text{Se}-$ and the other as isolated molecules SeO_n ($n = 1, 2, 3$) and/or related crystallites.

The figure shows that H-Se-O-Se-H and H-Se-O-Se clusters have the HOMO levels just above (≤ 0.5 eV) that of H-3Se-H. These level rises reflect stronger second-nearest interaction between the LP states of Se atoms in the Se-O-Se sequences, which results from two kinds of structural modifications. One is shorter distances (3.20 and 3.14 Å) between the Se atoms in Se-O-Se than that (3.74 Å)

in Se-Se-Se. The other is greater bond angles (119 and 122°) of Se-O-Se than that (106°) of Se-Se-Se, which enhance the parallelness of the LP wavefunctions in the triangular planes of Se-Se(O)-Se. We also note that, in these structures, O is negatively charged (-0.4) and, in response, the neighbouring Se atoms become slightly positive ($+0.2$) for compensation.

In Se solids, however, it seems that these HOMO levels hardly exert noticeable effects upon hole transport. The levels probably merge into the valence band, the width being strongly affected by the inter-chain interaction (discussed in 4.1), which is effective also in O-included chains. Actually, in a stacked structure (as that in Fig. 5) consisting of H-Se-O-Se-H and H-2Se-H with an inter-cluster separation of 3.5 Å, the HOMO level governed by Se π^* orbitals has shifted up to -6.4 eV, nearly overlapping the O-related ones.

On the other hand, we see in Fig. 9 that the LUMO level in H-Se-O-Se is located at mid-gap, in a similarly way to that in H-3Se. However, the existence of neutral Se dangling bonds in un-excited a-Se has been dismissed, as described in 2.1.

By contrast, ESR studies [72-74] have given firm evidence that the O dangling bond can exist. And, we see in the figure that H-2Se-O exhibits a slightly higher LUMO level (at -4 eV) than that of H-Se-O-Se, which reflects stronger ionic interaction in the terminal $-\text{Se}(+0.4)-\text{O}(-0.4)$ structure. Such a structure is assumed to work as a deep (~ 1 eV) trap for electrons, which may be responsible for the decrease in the electron lifetime (Table 1). However, the electron mobility is much smaller than that of holes (Table 1), and accordingly, no practical effects on the total electrical conductivity will appear. By constast, the O dangling bond is likely to contribute to the below-gap residual optical absorption in contaminated a-Se (Fig. 2) and in stressed hexagonal crystals [1].

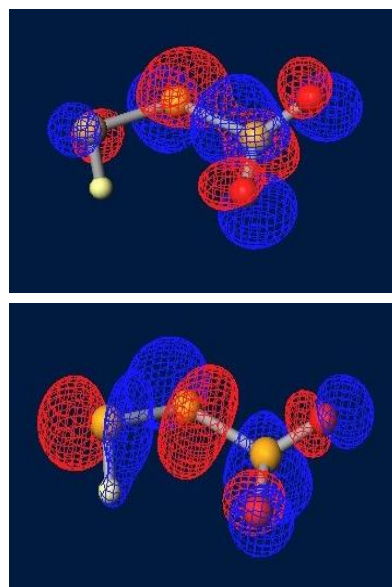


Fig. 11. Wavefunctions of LUMO (upper) and HOMO (lower) states in a stabilized H-3Se=2O cluster.

Incidentally, charged clusters H-2Se-O(\pm) exhibit some similarities to H-3Se(\pm). As shown in Fig. 9, the positive and the negative clusters have occupied and unoccupied levels in the HOMO-LUMO gap of H-3Se-H. The total energy of a H-2Se-O(+) plus H-2Se-O(-) pair is higher than that of a H-Se-O-2Se-O-Se-H chain by ~ 0.7 eV (without the dielectric correction), and accordingly, we are apt to envisage the existence.

Se chains can be terminated also by dual and triple O atoms, since the atom is smaller. Here, it seems interesting to examine variations in the terminal -Se-O, -Se=2O (Fig. 11), and -Se \equiv 3O. The calculation has demonstrated that, in these structures, each O charge is kept constant at $-0.4 \sim -0.5$, and corresponding to the O number of 1, 2 to 3, compensating Se charges increase from $+0.4, +0.7$ to $+1.1$. In addition, as shown in Fig. 9, the LUMO levels of H-2Se-O, =2O and \equiv 3O shift to lower values from $-4.0, -5.6$ eV to -6.3 eV. And, it is plausible that the LUMO level (with the wavefunction shown in Fig. 11) of -Se=2O, the existence in g-Se being experimentally demonstrated [46], distributes at ~ 0.5 eV above the top of the valence band in Se solids. These conditions are favorable to produce conspicuous isoelectronic impurity effects, letting the Se atom behave as an acceptor, the idea being proposed by MacKenzie [47]. Such structures may be responsible for the dramatic resistivity drop in Fig. 1 and also for sources of low-voltage avalanche breakdown [108]. (To the author's knowledge, however, no studies have been reported for avalanching behaviors in intentionally O-doped Se samples.)

It is mentioned here that other O-included clusters appear unstable. For instance, O \equiv 3(SeH) decomposed to H-Se-O-Se-H and H-Se, in a similar way to the three-fold coordinated Se. Also, H-Se=2O=Se-H divided into a pair of H-Se-O clusters.

On the other hand, SeO $_n$ ($n = 1, 2, 3$) molecules seem to have little electrical while appreciable optical effects. The calculation has demonstrated that in these molecules, with increases in n , the Se-O length shortens from 1.67 to 1.62 Å, in consistent with a previous analysis [109], and the Se charge increases from $+0.3$ to $+1.3$. These changes contribute to the widening of the HOMO-LUMO gaps, as shown in Fig. 9, from ~ 1 to ~ 5 eV. In consequence, SeO is likely to behave as a molecular absorption center, while SeO $_2$ and SeO $_3$ may cause mid-gap absorption in Se matrices. Finally, it should be mentioned that recent vibrational studies [109,110] reinforce the existence of molecular and crystalline forms of SeO $_2$ (100 ppm levels) in g-Se [46,47,68]. However, to the author's knowledge, electronic structures of crystalline SeO $_2$, consisting of -O-(Se=O)-O- chains, have hardly been known [111], and accordingly, its role cannot be explored.

4.5. As incorporation

Why is the O-impurity effect prominent only in elemental Se? For instance, As $_2$ Se $_3$ appears to be relatively insensitive to O inclusion [87,112]. In addition, what is the

reason for the compensation effects of, e.g., As in O-contaminated Se, mentioned in 2.1 ?

These features are understandable taking three features, shown in Fig. 12, into account: First, in comparing As-O and As-Se(S, Te) bonds, the former is more ionic and stronger [3,4,113]. Actually, we see in the figure that the As charge in As \equiv (OH) $_3$ is nearly 4. Accordingly, As-O bonds are preferred in As-doped, oxygenated Se. Second, the LUMO levels of As \equiv (OH) $_x$ (SeH) $_{3-x}$ clusters, which are located at higher energies than that of H-4Se-H, become progressively higher with x . Third, the HOMO levels of these As-clusters lie at similar energies to that of H-4Se-H, with the charge of Se remaining almost 4, irrespective of the O inclusions. Hence, in a-Se, the HOMO levels tend to overlap with the valence band, causing little appreciable effects. In short, these three conditions can explain the compensation effect of As in O-contaminated Se and also little O effects in As $_2$ Se $_3$.

Otherwise, in more details, we see in Fig. 12 that the As \equiv (SeH) $_3$ cluster has a slightly higher (~ 0.5 eV) HOMO level than that in H-4Se-H chains. This result implies that the As doping into pure Se, the process that is routinely employed for preparing stabilized a-Se films [34,58,60] having improved thermal stability [3], tends to produce shallow hole traps, giving rise to reduction of the hole mobility. Lastly, it should be mentioned that the calculation has also demonstrated similar results for Si doping in O-contaminated Se, in accordance with experimental results [47].

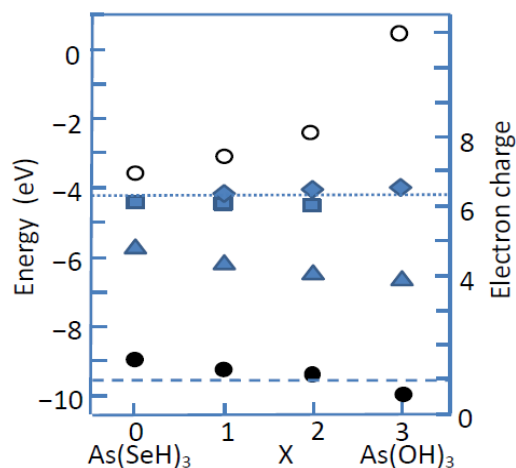


Fig. 12. HOMO (\bullet) and LUMO (\circ) energies of As \equiv (OH) $_x$ (SeH) $_{3-x}$ clusters in comparison with those (dashed and dotted lines) of H-4Se-H, calculated by PM3. Also shown at the right-hand side scale are the valence electron charges of As (\blacktriangle), O (\blacklozenge), and Se (\blacksquare). The electron charge of H is kept within 1 ± 0.1 .

4.6. Isoelectronic doping

In concluding this section, it may be valuable to reconsider the roles of doping in crystalline and amorphous semiconductors. For the former, the mechanism of atomic

doping has been documented [114]; e.g., P-doping in crystalline Si, in which *substitutional* P atoms behaves as donors, is ascribed to the valence number of 5, which is different from the coordination number 4 of the Si matrix. However, in amorphous semiconductors, e.g., P-doped a-Si:H, the doping efficiency is considerably suppressed, since the matrix is more flexible and P atoms can covalently be five-fold coordinated. Such coordination flexibility explains why, in general, impurity effects upon electrical conduction are less conspicuous in amorphous semiconductors [2, 4].

In this respect, the isoelectronic doping [114,115] of O atoms into Se is exceptional due to the two characteristics. One is, not the coordination number, but marked ionicity difference causes the doping effect. Actually, the calculation has demonstrated that insertion of S and Te, instead of O, into H-Se-Se(O,S,Te)-Se-H clusters produces much smaller electronic effects, which are consistent with previous observations [18,55,64-67]. In addition, we have seen the importance of paired O doping, as $-\text{Se}=\text{2O}$, which is favoured by the small size of O atoms.

5. Summaries

After a brief review of gap-state related properties in non-crystalline Se, we have considered responsible atomic structures through simple molecular-orbital calculations. Among various structural variations in H-*n*Se-H chains, the HOMO energy is considerably affected by the dihedral angle and the inter-molecular separation, which may cause hole traps. By contrast, the LUMO energy substantially varies with the chain length *n*, and its fluctuation can produce electron traps. Small ring molecules such as Se₄ have narrow HOMO-LUMO gaps. Isolated defective bonds, neutral or charged, could produce midgap states, while the existence is very limited. By contrast, intimate valence-alternation pairs are likely to behave as shallow hole traps.

The calculation has also demonstrated that, when O is included into Se chains as an impurity, it exhibits varied behaviors. Specifically interesting is the isoelectronic impurity effect of chain-terminating paired O atoms, $-\text{Se}=\text{2O}$, the structure which probably behaves as an acceptor. Such O-impurity effects, however, can be compensated by addition of As, through producing more stable As-O bonds.

Finally, it should be noted that many defect- and impurity-related problems in non-crystalline Se remain unresolved. For instance, why the resistivity becomes mostly constant for the O concentration above ~10 ppm (Fig. 1) is speculative. For elucidating the role of O atoms, we require one-to-one corresponding data of electrical conductivity, optical (visible and IR) absorption, and so forth for series of O-doped Se samples. In addition, structures and properties should be comparatively examined for glassy and amorphous Se samples in more details.

Acknowledgement

The author would like to thank Professor K. Shimakawa for critical reading and valuable comments.

References

- [1] R.A. Zingaro, W.C. Cooper (eds.), Selenium (Van Nostrand Reinhold Company, New York, 1974).
- [2] N.F. Mott, E.A. Davis, Electronic Processes in Non-Crystalline Materials (Clarendon Press, Oxford, 1979).
- [3] M. Popescu, Non-Crystalline Chalcogenides (Kluwer Academic Pub. Dordrecht, 2000).
- [4] K. Tanaka, K. Shimakawa, Amorphous Chalcogenide Semiconductors and Related Materials (Springer, New York, 2011).
- [5] S. Kasap, J.B. Frey, G. Belev, O. Tousignant, H. Mani, J. Greenspan, L. Laperriere, O. Budon, A. Reznik, G. DeCrescenzo, K.S. Karim, J.A. Rowlands, Sensors **11**, 5112 (2011).
- [6] T. Masuzawa, S. Kuniyoshi, M. Onishi, R. Kato, I. Saito, T. Yamada, A.T.T. Koh, D.H.C. Chua, T. Shimosawa, Appl. Phys. Lett. **102**, 073506 (2013).
- [7] J.R. Goldan, A.H. Goldan, O. Tousignant, S. Leveille, W. Zhao, Med. Phys. **42**, 1223 (2015).
- [8] D.S. Deng, N.D. Orf, S. Danto, A.F. Abouraddy, J.D. Joannopoulos, Y. Fink, Appl. Phys. Lett. **96**, 023102 (2010).
- [9] A. Saitoh, H. Takebe, K. Tanaka, J. Optoelectron. Adv. Mater. **13**, 1524 (2011).
- [10] S. Sinha, S.K. Chatterjee, J. Ghosh, A.K. Meikap, J. Appl. Phys. **113**, 123704 (2013).
- [11] R. Zhang, X. Tian, L. Ma, C. Yang, Z. Zhou, Y. Wang, S. Wang, RSC Adv. **5**, 45165 (2015).
- [12] A. von Hippel, J. Chem. Phys. **16**, 372 (1948).
- [13] V.S. Minaev, S.P. Timoshenkov, V.V. Kalugin, J. Optoelectron. Adv. Mater. **7**, 1717 (2005).
- [14] S.N. Yannopoulos, K.S. Andrikopoulos, Phys. Rev. B **69**, 144206 (2004).
- [15] T. Scopigno, W. Steurer, S.N. Yannopoulos, A. Chrissanthopoulos, M. Krisch, G. Ruocco, T. Wagner, Nat. Commun. **2**, 195 (2011).
- [16] J. Mort, J. Appl. Phys. **39**, 3543 (1968).
- [17] R.J.F. Dalrymple, W.E. Spear, J. Phys. Chem. Solids **33**, 1071 (1972).
- [18] W.D. Gill, G.B. Street, J. Non-Cryst. Solids **13**, 120 (1973/74).
- [19] R.A. Street, N.F. Mott, Phys. Rev. Lett. **35**, 1293 (1975).
- [20] M. Kastner, D. Adler, H. Fritzsche, Phys. Rev. Lett. **37**, 1504 (1976).
- [21] D. Vanderbilt, J.D. Joannopoulos, Phys. Rev. B **27**, 6311 (1983).
- [22] S. Itoh, K. Nakao, J. Phys. C: Solid State Phys. **17**, 3373 (1984).

- [23] C.K. Wong, G. Lucovsky, J. Bernholc, *J. Non-Cryst. Solids* **97&98**, 1171 (1987).
- [24] M. Springborg, R.O. Jones, *J. Chem. Phys.* **88**, 2652 (1988).
- [25] A. Ikawa, H. Fukutome, *J. Phys. Soc. Jpn.* **58**, 4517 (1989).
- [26] A. Ikawa, H. Fukutome, *J. Phys. Soc. Jpn.* **59**, 1002 (1990).
- [27] T. Koslowski, *J. Phys.: Condens. Matter* **9**, 613 (1997).
- [28] D. Molina, E. Lomba, G. Kahl, *Phys. Rev. B* **60**, 6372 (1999).
- [29] X. Zhang, D.A. Drabold, *Phys. Rev. Lett.* **83**, 5042 (1999).
- [30] G. Kresse, F. Kirchhoff, M.J. Gillan, *Phys. Rev. B* **59**, 3501 (1999).
- [31] S.A. Dembovsky, *J. Non-Cryst. Solids* **353**, 2944 (2007).
- [32] F.V. Grigor'ev, *Russ. J. Inorg. Chem.* **54**, 260 (2009).
- [33] C. Oligschleger, C. Facius, H. Kutz, C. Langen, M. Thumm, S. von Brühl, S. Wang, L. Weber, J. Zischler, *J. Phys.: Condens. Matter* **21**, 405402 (2009).
- [34] J. Berashevich, A. Mishchenko, A. Reznik, *Phys. Rev. Appl.* **1**, 034008 (2014).
- [35] M. Mastsui, *J. Phys. Chem. C* **118**, 19294 (2014).
- [36] S.R. Ovshinsky, D. Adler, *Contemp. Phys.* **19**, 109 (1978).
- [37] H. Fritzsche, *Proc. 7th Int. Conf. Am. Liq. Semicond.*, W.E. Spear (ed.) (Centre for Industrial Consultancy and Liaison, 1977) pp. 3-15.
- [38] F. Eckart, *Ann. Phys.* **14**, 233 (1954).
- [39] P.T. Kozyrev, *Sov. Phys.- Solid State* **1**, 102 (1959).
- [40] G.B. Abdullaev, G.M. Aliev, Kh.G. Barkinkhoev, Ch.M. Askerov, L.S. Larionkina, *Sov. Phys.-Solid State* **6**, 786 (1964).
- [41] G.B. Abdullaev, S.I. Mekhtieva, G.M. Aliev, D. Sh. Abdinov, T.G. Kerimova, *Phys. Stat. Sol.* **16**, K31 (1966).
- [42] O. Oda, A. Onozuka, I. Tsuboya, *J. Non-Cryst. Solids* **83**, 49 (1986).
- [43] M. Abkowitz, S.S. Badesha, F.E. Knier, *Solid St. Commun.* **57**, 579 (1986).
- [44] J.L. Hartke, *Phys. Rev.* **125**, 1177 (1962).
- [45] B.G. Bagley, F.J. DiSalvo, J.V. Waszczak, *Solid St. Commun.* **11**, 89 (1972).
- [46] R.A. Burley, *Phys. Stat. Sol.* **29**, 551 (1968).
- [47] J.D. MacKenzie, *J. Non-Cryst. Solids* **2**, 16 (1970).
- [48] B. Voigt, G. Dresler, *Analytica Chimica Acta* **127**, 87 (1981).
- [49] T. Obata, B. Tsujimura, O. Oda, *Surf. Sci.* **135**, 110 (1983).
- [50] K. Suzuki, K. Matsumoto, H. Hayata, N. Nakamura, N. Minari, *J. Non-Cryst. Solids* **95&96**, 555 (1987).
- [51] X. Yang, Y. Hu, S. Yang, M.M.T. Loy, *J. Chem. Phys.* **111**, 7837 (1999).
- [52] C. Bréchnignac, Ph. Cahuzac, N. Kébaïli, J. Leygnier, *J. Chem. Phys.* **112**, 10197 (2000).
- [53] K. Kooser, D.T. Ha, E. Itälä, J. Laksman, S. Urpelainen, E. Kukkk, *J. Chem. Phys.* **137**, 044304 (2012).
- [54] K. Weimer, *Phys. Rev.* **79**, 171 (1950).
- [55] P.H. Keck, *J. Opt. Soc. Am.* **42**, 221 (1952).
- [56] J.L. Hartke, *Phys. Rev.* **125**, 1177 (1962).
- [57] M.M. Abdul-Gader, M.A. Al-Basha, K.A. Wishah, *Int. J. Electronics* **85**, 21 (1998).
- [58] R.E. Johanson, S.O. Kasap, J. Rowlands, B. Polischuk, *J. Non-Cryst. Solids* **227-230**, 1359 (1998).
- [59] W.C. Lacourse, V.A. Twaddell, J.D. MacKenzie, *J. Non-Cryst. Solids* **3**, 234 (1970).
- [60] G. Belev, D. Tonchev, B. Fogal, C. Allen, S.O. Kasap, *J. Phys. Chem. Solids* **68**, 972 (2007).
- [61] J.C. Bernède, G. Safoula, A. Ameziane, P. Burgaud, *Phys. Stat. Sol. (a)* **110**, 521 (1988).
- [62] V.A. Twaddell, W.C. LaCourse, J.D. McKenzie, *J. Non-Cryst. Solids* **8-10**, 831 (1972).
- [63] P.W. McMillan, S.D. Shutov, *J. Non-Cryst. Solids* **24**, 307 (1977).
- [64] J. Schottmiller, M. Tabak, G. Lucovsky, A. Ward, *J. Non-Cryst. Solids* **4**, 80 (1970).
- [65] M.K. El-Mously, M.M. El-Zaidia, *J. Non-Cryst. Solids* **11**, 519 (1973).
- [66] M.F. Kotkata, A.F. El-Dib, *Mater. Sci. Engn.* **67**, 39 (1984).
- [67] M.M. El-Nahass, M.A.M. Seyam, H.E.A. El-Sayed, A.M. Abd El-Barry, *Appl. Surf. Sci.* **252**, 6218 (2006).
- [68] A. Vaško, D. Ležal, I. Srb, *J. Non-Cryst. Solids* **4**, 31 (1970).
- [69] K. Tanaka, S. Nakayama, *Jpn. J. Appl. Phys.* **38**, 3986 (1999).
- [70] K. Tanaka, T. Gotoh, N. Yoshida, S. Nonomura, *J. Appl. Phys.* **91**, 125 (2002).
- [71] K. Tanaka, *J. Non-Cryst. Solids* **426**, 32 (2015).
- [72] G.B. Ablullaev, N.I. Ibragimov, Sh. V. Mamedov, T. Ch. Zhuvarly, *Phys. Stat. Sol.* **18**, K113 (1966).
- [73] P.I. Sampath, *J. Chem. Phys.* **45**, 3519 (1966).
- [74] I. Chen, *J. Chem. Phys.* **45**, 3536 (1966).
- [75] M. Abkowitz, *J. Chem. Phys.* **46**, 4537 (1967).
- [76] B.G. Bagley, F.J. DiSalvo, J.V. Waszczak, *Solid St. Commun.* **11**, 89 (1972).
- [77] S.C. Agarwal, *Phys. Rev. B* **7**, 685 (1973).
- [78] W.W. Warren, Jr., R. Dupree, *Phys. Rev. B* **22**, 2257 (1980).
- [79] P. Nielsen, *Solid St. Commun.* **9**, 1745 (1971).
- [80] J. Mort, A.I. Lakatos, *J. Non-Cryst. Solids* **4**, 117 (1970).
- [81] S.G. Bishop, U. Strom, P.C. Taylor, *Phys. Rev. B* **15**, 2278 (1977).
- [82] A.V. Kolobov, M. Kondo, H. Oyanagi, A. Matsuda, K. Tanaka, *Phys. Rev. B* **58**, 12004 (1998).
- [83] R.A. Street, *Adv. Phys.* **25**, 397 (1976).
- [84] V.I. Mikla, V.V. Mikla, *J. Mater. Sci.: Mater. Electron.* **20**, 1059 (2009).

- [85] K. Koughia, S.O. Kasap, *J. Non-Cryst. Solids* **352**, 1539 (2006).
- [86] G.J. Adriaenssens, M.L. Benkheldir, *J. Non-Cryst. Solids* **354**, 2687 (2008).
- [87] S.G. Bishop, U. Strom, P.C. Taylor, *The Physics of Selenium and Tellurium*, E. Gerlach and P. Grosse (eds.) (Springer-Verlag, Berlin, 1979) pp. 193-202.
- [88] B.T. Kolomiets, T.N. Mamontova, A.V. Chernyshov, G.Z. Vinogradova, N.V. Demokritova, *Phys. Stat. Sol. (a)* **79**, K89 (1983).
- [89] J.J.P. Stewart, *J. Comput. Chem.* **10**, 209 (1989).
- [90] M.W. Schmidt, K.K. Baldrige, J.A. Boatz, S.T. Elbert, M.S. Gordon, J.H. Jensen, S. Koseki, N. Matsunaga, K.A. Nguyen, S.J. Su, T.L. Windus, M. Dupuis, J.A. Montgomery, *J. Comput. Chem.* **14**, 1347 (1993).
- [91] <http://winmostar.com/jp/>
- [92] C. -G. Zhan, J.A. Nichols, D.A. Dixon, *J. Phys. Chem. A* **107**, 4184 (2003).
- [93] D.G. Streets, J. Berkowitz, *J. Electron Spec. Related Phenomena* **9**, 269 (1976).
- [94] K. Blasubramanian, M.Z. Liao, M. Han, *Chem. Phys. Lett.* **139**, 551 (1987).
- [95] J.T. Snodgrass, J.V. Coe, K.M. McHugh, C.B. Freidhoff, K.H. Bowen, *J. Phys. Chem.* **93**, 1249 (1989).
- [96] P. Jensen, I.N. Kozin, *J. Mol. Spectro.* **160**, 39 (1993).
- [97] L. Pisani, E. Clementi, *J. Chem. Phys.* **101**, 3079 (1994).
- [98] M. Ehara, M. Ishida, H. Nakatsuji, *J. Chem. Phys.* **114**, 8990 (2001).
- [99] NIST-Chem. Web., <http://webbook.nist.gov/chemistry>.
- [100] S. T. Gibson, J. P. Greene, J. Berkowitz, *J. Chem. Phys.* **85**, 4815 (1986).
- [101] Z.Q. Li, J.Z. Yu, K. Ohno, B.L. Gu, R. Czajka, A. Kasuya, Y. Nishina, Y. Kawazoe, *Phys. Rev. B* **52**, 1524 (1995).
- [102] C. Heinemann, W. Koch, G.-G. Lindner, D. Reinen, P.-O. Widmark, *Phys. Rev. A* **54**, 1979 (1996).
- [103] W. Xu, W. Bai, *J. Mol. Str. THEOCHEM* **854**, 89 (2008).
- [104] A. Alparone, *Theor. Chem. Acc.* **131**, 1239 (2012).
- [105] P. Andonov, *J. Non-Cryst. Solids* **47**, 297 (1982).
- [106] S. Kohara, A. Goldbach, N. Koura, M.-L. Saboungi, L.A. Curtiss, *Chem. Phys. Lett.* **287**, 282 (1998).
- [107] B.C. Pan, J.G. Han, J. Yang, S. Yang, *Phys. Rev. B* **62**, 17026 (2000).
- [108] K. Tanaka, *J. Opt. Adv. Mater.* **16**, 243 (2014).
- [109] W. Xu, W. Bai, *J. Mol. Str. THEOCHEM* **863**, 1 (2008).
- [110] R.J.M. Konings, A.S. Booij, A. Kovács, *Chem. Phys. Lett.* **292**, 447 (1998).
- [111] K. Tripathi, M. Husain, M. Zulfequar, *Chalcogenide Lett.* **6**, 517 (2009).
- [112] M. Hammam, G.J. Adriaenssens, J. Dauwen, G. Seynhaeve, W. Grevendonk, *J. Non-Cryst. Solids* **119**, 89 (1990).
- [113] R.A. Street, G. Lucovsky, *Solid St. Commun.* **31**, 289 (1979).
- [114] J.C. Phillips, *Bonds and Bands in Semiconductors* (Academic Press, New York, 1973), Chap. 9.
- [115] C.A. Londos, E.N. Sgourou, A. Chroneos, *J. Mater. Sci.: Mater. Electron.* **24**, 1696 (2013).

*Corresponding author: keiji@eng.hokudai.ac.jp